Journal of Insights in Basic and Applied Sciences
مجلة رؤى في العلوم الأساسية والتطبيقية
Volume 2, Issue 3, 2026, Pages: 13-26
Journal homepage: https://jibas.com.ly/index.php/jibas/en

Nano-Engineered Interfaces and Charge Transport Layers in Perovskite Solar Cells: Progress, Degradation Dynamics, and Future Scalability

Rahma Elzer[1 *], Abdulgader Alsharif [2]
[1] Department of Physics, Faculty of Science, University of Derna, Derna, Libya
[2] Department of Electrical and electronic engineering, College of Technical Science Sabha, Sabha, Libya

الواجهات النانوية المهندسة وطبقات نقل الشحنة في خلايا البيروفسكايت الشمسية: التقدم، ديناميكيات التدهور، وقابلية التوسع المستقبلية

رحمة الزير [1*]، عبدالقادر الشريف [2]
[1] قسم الفيزياء، كلية العلوم، جامعة درنة، درنة، ليبيا
[2] قسم الهندسة الكهربائية والإلكترونية، كلية العلوم التقنية سبها، سبها، ليبيا

*Corresponding author: rahmaelzer454@gmail.com

Received: May 20, 2026	Accepted: June 25, 2026	Published: July 02, 2026

Abstract:
Nano-engineered interfaces and charge transport layers (CTLs) have become fundamental to the advancement of perovskite solar cells (PSCs) due to their simultaneous control over carrier selectivity, interfacial recombination, and operational durability. This critical review systematically evaluates the efficiency-stability trade-off governed by nanostructured transport matrices, emphasizing how interfacial energy alignment, defect density, and mechanical mismatch collectively dictate device behavior under real-world operating conditions. Particular attention is devoted to coupled degradation cascades, including field-driven ion and defect migration along grain boundaries, trap-assisted non-radiative recombination pathways, chemical corrosion and volatilization at reactive boundaries, and thermomechanical modulus mismatches induced by diurnal thermal cycling. Furthermore, this review dissects recent milestones in nano-engineered electron and hole transport materials configured to mitigate these losses through optimized band alignment and enhanced interface selectivity. We highlight quantum-confined tin dioxide SnO_2 quantum dots (QDs) for their ideal conduction band minimum (CBM) matching with the perovskite layer, enabling downhill electron extraction while providing a robust hole-blocking barrier. Concurrently, homogenized nickel oxide NiO_x nanoparticles, specifically m-NiO_x, are evaluated as promising hole-selective contacts. The deeper valence band maximum (VBM) of m-NiO_x (≈ –5.36 eV versus –5.22 eV in conventional c-NiO_x) offers a superior energetic match with the perovskite valence edge, accelerating hole extraction and improving electron blocking. A forward-looking roadmap is outlined, focusing on Machine Learning (ML)-assisted screening of interfaces, standardized multi-stress stability tracking under ISOS protocols, and eco-friendly scalable manufacturing.

Keywords: Perovskite solar cells; Nano-engineered interfaces; Charge transport layers; Interfacial degradation; Scalable manufacturing.

الملخص

أصبحت الواجهات النانوية المهندسة وطبقات نقل الشحنة (CTLs) أساسية لتطوير خلايا البيروفسكايت الشمسية (PSCs) نظرًا لتحكمها المتزامن في انتقائية الناقلات، وإعادة التركيب البيني، والمتانة التشغيلية. يستعرض هذا البحث النقدي بشكل منهجي المقايضة بين الكفاءة والاستقرار التي تحكمها المصفوفات النانوية المهندسة، مع التركيز على كيفية تحديد محاذاة الطاقة البينية، وكثافة العيوب، وعدم التوافق الميكانيكي مجتمعة لسلوك الجهاز تحت ظروف التشغيل الواقعية. يُولى اهتمام خاص لسلسلة التدهور المترابطة، بما في ذلك هجرة الأيونات والعيوب الناتجة عن المجال على طول حدود الحبوب، ومسارات إعادة التركيب غير الإشعاعي بمساعدة الفخاخ، والتآكل الكيميائي والتطاير عند الحدود التفاعلية، وعدم توافق المعامل الحراري الميكانيكي الناتج عن الدورات الحرارية اليومية. علاوة على ذلك، يحلل هذا البحث الإنجازات الأخيرة في مواد نقل الإلكترون والثقوب النانوية المهندسة والمصممة للتخفيف من هذه الخسائر من خلال تحسين محاذاة النطاقات وتعزيز انتقائية الواجهة. نسلط الضوء على نقاط الكم من SnO_2 المحصورة كميًا لتطابقها المثالي مع الحد الأدنى لنطاق التوصيل (CBM) مع طبقة البيروفسكايت، مما يتيح استخراج الإلكترونات بانحدار هابط مع توفير حاجز قوي لحجب الثقوب. في الوقت نفسه، يتم تقييم جسيمات أكسيد النيكل NiO_x النانوية المتجانسة، وتحديدًا m-NiO_x، كتماسات انتقائية للثقوب واعدة. يوفر الحد الأقصى لنطاق التكافؤ (VBM) الأعمق لـ m-NiO_x (≈ –5.36 eV مقابل –5.22 eV في c-NiO_x التقليدي) تطابقًا طاقيًا متفوقًا مع حافة تكافؤ البيروفسكايت، مما يسرع استخراج الثقوب ويحسن حجب الإلكترونات. يتم تحديد خارطة طريق استشرافية تركز على الفحص بمساعدة التعلم الآلي (ML) للواجهات، وتتبع الاستقرار القياسي متعدد الإجهاد وفق بروتوكولات ISOS، والتصنيع القابل للتوسع الصديق للبيئة.

الكلمات المفتاحية: خلايا البيروفسكايت الشمسية؛ الواجهات النانوية المهندسة؛ طبقات نقل الشحنة؛ التدهور البيني؛ التصنيع القابل للتوسع.

Introduction

Perovskite solar cells (PSCs) have advanced from early proof-of-concept devices to power conversion efficiencies exceeding 26% in conventional architectures and surpassing 27% in inverted structures, positioning them among the most competitive thin-film photovoltaic platforms (Qin et al., 2024). Yet the central obstacle has shifted from efficiency acquisition to efficiency retention under realistic operating conditions, because device lifetimes remain well below the requirements for commercial deployment(Qin et al., 2024)) X. Liu et al., 2026; Zang et al., 2024(. This tension has made stability, rather than peak performance, the defining problem for the present phase of perovskite photovoltaics(Berhe et al., 2016; Nazir et al., 2022) .

Degradation pathways propagate across the entire device architecture, encompassing the perovskite absorber, the electron transport layer (ETL), the hole transport layer (HTL), and their respective heterojunctions (Shen et al., 2024; Shi et al., 2026; Wei et al., 2021). Consequently, these continuous interfaces represent primary failure zones where defect chemistry, ion redistribution, energetic misalignment, and thermomechanical strain concentrate under simultaneous operational stressors (J. Chen et al., 2025; Shen et al., 2024; Shi et al., 2026) . Transport layers can no longer be evaluated merely as passive, charge-selective contacts; instead, they function as electronically, chemically, and mechanically active components that directly govern both the degradation kinetics and stabilization mechanisms of the photovoltaic device.

This interdependence is particularly evident at the perovskite/ETL interface. Recombination losses at this junction remain a recognized performance bottleneck, while ETL defects, pinholes, hydroxyl-rich surfaces, and poor band alignment can accelerate oxygen diffusion, charge accumulation, ion migration, and interfacial decomposition (Gong, Cui, Li, & Liu, 2023; Zang et al., 2024). Even when inorganic ETLs such as SnO_2, TiO_2, ZnO, and related nanostructures offer superior optical transparency and nominal thermodynamic stability, their practical effect depends on morphology, surface chemistry, and the quality of the contact they form with the perovskite (Gong et al., 2023; Zang et al., 2024). Studies on flexible devices sharpen this argument: incomplete coverage in colloidal SnO_2 nanoparticle layers can generate shunting pathways and current crowding, directly linking nanoscale film nonuniformity to long-term operational loss(K. W. Kim et al., 2024) . At the same time, the ETL can influence the electronic and ionic behavior of remote layers, altering hysteresis, recombination, and even the resistance and capacitance of the HTL(Hermes, Hou, Bergmann, Brabec, & Weber, 2018) .

An analogous, though not identical, problem exists at the perovskite/HTL interface. Widely used organic HTLs have enabled high efficiencies, yet they often suffer from limited photochemical stability and dopant diffusion during operation, while some bottom-contact HTLs can actively induce decomposition of the adjacent perovskite under illumination (Elnaggar et al., 2020; Wei et al., 2021). By contrast, inorganic HTLs such as NiO_x and related compounds have attracted sustained interest because their intrinsic chemical robustness and suitable energetics can improve ambient stability, although their interfacial chemistry is not automatically benign and still requires deliberate control (Kung et al., 2018). Recent work has made the broader lesson more explicit: heterointerface durability is governed by a trade-off between bonding and degradation, where stronger interfacial interactions can improve adhesion yet also intensify proton-transfer-driven chemical instability if the interface is improperly designed (J. Chen et al., 2025). This is why mechanical integrity, often treated as secondary to electronic

alignment, must be integrated into any serious account of transport-layer-mediated stability(Gong et al., 2023; Shen et al., 2024) .
Nanomaterial-based transport layers have emerged as a compelling route to address these intertwined limitations because nanoscale composition, dimensionality, and surface functionality can be used to tune extraction selectivity, defect passivation, interfacial adhesion, and barrier properties simultaneously (Wang et al., 2026; Zang et al., 2024; Zhou, Duan, Duan, & Tang, 2022). The literature already shows that replacing unstable organic contacts with solution-processed metal-oxide layers can markedly improve resistance to water and oxygen, and that interface-stabilizing interlayers such as 2D capping layers can extend operational lifetimes to thousands of hours under accelerated stress(You et al., 2016; Zhao et al., 2022) . Yet the field has not converged on a single materials solution. Some inorganic charge transport layers still underperform their organic counterparts because reduced interface quality, contradictory interfacial chemistries, and suboptimal extraction persist despite the apparent advantage of higher bulk stability(X. Liu et al., 2026) .
Against this background, a critical review of nanomaterial-based ETLs and HTLs is timely not because the field lacks candidate materials, but because it still lacks a sufficiently discriminating framework for relating nanomaterial choice to specific degradation pathways. Such a framework must account for how transport layers regulate defect populations, ion migration, interfacial recombination, environmental ingress, electrode reactions, and chemo-mechanical failure across both n-i-p and p-i-n architectures (Gong et al., 2023; Paul et al., 2026; Wang et al., 2026). It must also distinguish genuine interface stabilization from apparent short-term efficiency gains that mask latent instability. The purpose of this review is therefore to examine nanomaterial-based electron and hole transport layers not as isolated functional films, but as interfacial systems whose electronic structure, chemistry, morphology, and mechanical coupling collectively determine whether perovskite solar cells approach durable operation or remain trapped in accelerated decay.

2. Interfacial Degradation Mechanisms

Device performance decay under accelerated aging is predominantly initiated at the heterojunctions where the perovskite absorber meets the selective transport contacts, rather than within the bulk crystal lattice. These buried interfaces function as reactive zones where electrical, thermal, and environmental stressors converge to destabilize the complete device stack(N. Ahn & Choi, 2024) . Under continuous operation, the interplay between the internal built-in potential and operational temperature drives coupled ionic and structural transformations that progressively compromise the charge extraction efficiency of the selective contacts(N. Liu, Zhang, Liang, Xue, & Wang, 2023).

What makes these interfaces particularly vulnerable is their dual role: they must simultaneously facilitate efficient charge transfer while blocking unwanted chemical and ionic exchange. This inherent contradiction creates a perpetual tension that manufacturers have yet to fully resolve. The primary degradation pathways operating at these boundaries encompass four interconnected mechanisms, each feeding into and amplifying the others in a destructive feedback loop.

2.1 Field-Driven Defect and Ion Migration

Halide perovskites exhibit mixed ionic-electronic conductivity, characterized by notoriously low activation energies ($E_a \approx 0.1–0.6$ eV) for point defect migration, particularly iodine vacancies ($V\_I\bullet$) and interstitial iodide ions (I_i^-) (Kouroudis et al., 2024). Under sustained forward bias, the internal built-in potential drops across the device, stimulating volatile iodide species to drift dynamically along grain boundaries toward the anode, while positive organic cations (MA^+, FA^+) migrate toward the cathode. Crucially, this ionic redistribution does not merely respond passively to the electric field; it actively reconstructs the local electronic structure, establishing transient electrostatic barriers that persist even after bias removal—a phenomenon directly correlated with the anomalous J–V hysteresis and accelerated interfacial recombination observed in operational devices (Khadka, Shirai, Yanagida, & Miyano, 2021; Zai, Ma, Chen, & Zhou, 2021). This accumulation distorts the local vacuum level, induces severe energy band bending, and screens the built-in potential, thereby driving substantial interfacial charge trapping and pronounced J-V hysteresis (Khadka et al., 2021; Zai et al., 2021). Consequently, high efficiency under steady-state laboratory testing does not guarantee performance stability under dynamic, real-world operational fields.

2.2 Interfacial Non-Radiative Recombination Cascades

Unpassivated interfacial defects such as metallic lead (Pb^{2+}) clusters, under-coordinated halides, and oxygen vacancies on oxidized transition metal surfaces—introduce deep energy levels within the bandgap, driving intense

Shockley-Read-Hall (SRH) recombination (Z. Xu, Kerner, Kronik, & Rand, 2024). Photogenerated carriers escaping the bulk are lost at these surface states, directly capping the device's open-circuit voltage (V_oc) and fill factor (FF), pulling the junction far below its radiative thermodynamic limit (Wang et al., 2026).

The severity of SRH recombination at these interfaces is not solely determined by defect density; it is equally governed by the energetic alignment between the perovskite and the transport layer. A misalignment of even 0.2 eV can increase recombination current by an order of magnitude, underscoring the need for precise band engineering rather than merely defect passivation (Luo, Su, Zhang, Gong, & Zhu, 2020; Z. Xu et al., 2024). What complicates matters further is that the optimal alignment under dark conditions does not necessarily hold under illumination or bias, where ion redistribution and trapped charge can dynamically shift the local band edges.

Recent advances in surface passivation—including the deployment of organic ammonium salts, low-dimensional perovskite capping layers, and self-assembled monolayers—have yielded significant reductions in interfacial recombination (T. Jiang et al., 2024). However, the long-term sustainability of these improvements under operational stress remains a critical concern. Emerging studies indicate that the identical passivation agents engineered to mitigate surface defects can induce secondary instability pathways under prolonged thermal stress, driven by desorption, diffusion, or chemical reactions with the underlying perovskite lattice to form alternative defect states (T. Jiang et al., 2024). This paradox lies at the heart of the stability challenge.

2.3 Chemical Corrosion and Volatilization

Thermal stress forces volatile decomposition byproducts (e.g., HI, I_2, and CH_3NH_2 gas) to escape the perovskite lattice, initiating aggressive chemical reactions with adjacent layers (N. Ahn & Choi, 2024). Migrating iodine species (e.g., I^- and I_2) readily corrode conventional metal back-contacts such as Ag and Al, forming resistive interfacial layers of AgI and AlI_3 through a solid-state reaction that proceeds via iodine diffusion along grain boundaries, which exponentially increase series resistance (R_s) and contribute to irreversible performance loss (Guerrero et al., 2016; Paul et al., 2026). Conversely, hygroscopic organic additives like Li-TFSI continuously channel ambient moisture through soft film pinholes, driving the localized hydrolysis of the perovskite lattice into non-perovskite yellow phases (δ-$FAPbI_3$ or PbI_2) (W. Li et al., 2020; Zhou et al., 2022).

This chemical degradation is particularly insidious because it is self-accelerating. Once corrosion begins, the resulting byproducts—such as I_2 gas—can catalyze further decomposition in adjacent regions, effectively creating a propagating front of chemical attack. Recent work has shown that even a few tens of parts per million of oxygen can initiate photo-oxidation reactions that generate superoxide radicals, which then deprotonate organic cations and accelerate lattice collapse (Y. Wu et al., 2026). The implication is clear: chemical stability cannot be achieved through barrier layers alone; the perovskite itself must be intrinsically resistant to these reactions, or we are merely delaying the inevitable.

2.4 Thermomechanical Modulus Mismatch

Hybrid perovskites display a large linear coefficient of thermal expansion ($\alpha \approx 3 \times 10^{-5}\ K^{-1}$), whereas inorganic metal oxides are rigid lattices with vastly lower thermal expansion rates (Akylbayeva et al., 2026). Under diurnal thermal cycling (oscillating between −40°C and 85°C per ISOS protocols), this extreme thermomechanical mismatch concentrates severe shear strain at the buried heterojunction, ultimately causing mechanical delamination, micro-cracking, and a catastrophic loss of electrical contact (Khenkin et al., 2020) .

This failure mode receives considerably less attention than its chemical counterparts, yet it is arguably the most difficult to address through materials chemistry alone. Unlike ion migration or recombination, which can be partially mitigated through compositional tuning, thermomechanical failure is an intrinsic consequence of coupling two fundamentally dissimilar material classes. The challenge is compounded by the fact that mechanical stress is not distributed uniformly across the device; localized hotspots, thickness nonuniformities, and edge effects can amplify strain by orders of magnitude(Dai & Padture, 2023; Tirawat et al., 2024).

From an engineering perspective, this suggests that stability solutions cannot be confined to the materials level. Device architecture, contact geometry, and encapsulation strategies must all be co-optimized to accommodate the inevitable thermal expansion mismatch. Some promising work has explored the use of compliant interlayers or

stress-relief structures, but these approaches remain in their infancy and have yet to demonstrate durability under prolonged cycling.

2.5 The Interdependent Degradation Cascade

As conceptually illustrated in Figure 1, an elegant consensus has emerged that these individual mechanisms do not operate in isolation; rather, they form an interdependent degradation cascade (Boyd, Cheacharoen, Leijtens, & McGehee, 2018; Q. Jiang et al., 2023; Thiesbrummel et al., 2024). This is perhaps the most critical insight for understanding why perovskite solar cells fail, and why no single intervention has yet delivered the requisite decade-scale stability.

A standard cross-sectional configuration operating under forward bias and light experiences severe band bending, which traps photocarriers at localized interfacial energy dips (N. Ahn & Choi, 2024). This localized environment accelerates ion migration along the grain boundaries toward the defective transport junctions (Khadka et al., 2021; Zai et al., 2021). The resulting accumulation of mobile ions effectively screens the internal electric field, triggering rapid early-stage drops in short-circuit current density (J_{sc}) and fill factor (FF) that can easily outpace baseline trap-assisted recombination (Adhikari et al., 2025; Luo et al., 2020).

Simultaneously, unpassivated defect sites act as deep SRH recombination sinks, capping the V_{oc} (Adhikari et al., 2025; Luo et al., 2020), while illumination continuously drives the generation of negative iodide interstitials near the cathode interface, severely harming charge transport kinetics (Ni et al., 2022). This electronic decay is accompanied by severe chemical corrosion; escaping iodine species react with top metal back-electrodes (Ag/Au), forming insulating metal-iodide interphases and structural voids (Guerrero et al., 2016; Paul et al., 2026), alongside the volatilization of I_2 gas [30]. Finally, diurnal thermal cycling acts on the distinct lattice parameters of the adjacent materials, inducing substantial thermomechanical shear and localized fatigue micro-cracking along boundaries and scribes, resulting in permanent shunting and device failure) Ulicna et al., 2025; Wang et al., 2026(.

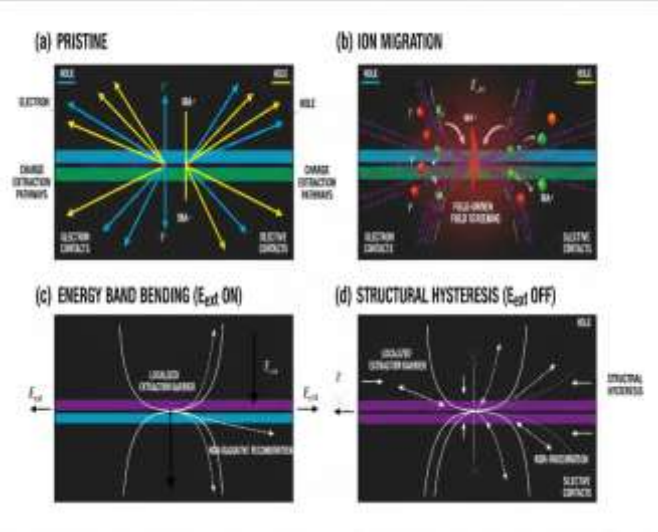

Figure 1: Schematic illustration of energy band alignment profiles at the selective contacts: (a) Quantum-confined CBM matching and hole-blocking dynamics at the modified SnO_2 QD electron-selective interface, showing the downward energetic cascade that facilitates electron extraction while the deep VBM blocks hole leakage. (b) Valence band engineering, Fermi level (E_F) position, and relative energetic extraction pathways of NiO_x NPs versus the multi-cation perovskite absorber bulk, contrasting the pristine NiO_x VBM (−5.3 eV) with the MeO-2PACz-modified NiO_x VBM (−5.7 eV).

The degradation mechanisms are summarized as follows. **Ion migration** occurs at grain boundaries and perovskite/CTL interfaces, driven by built-in potential, applied bias, and elevated temperature. It involves the migration of I^-, $V_{I^\bullet}$, MA^+, and FA^+ along grain boundaries, leading to field screening (E_{int}), charge accumulation, reduced J_{sc} and FF, severe J_V hysteresis, and unstable PCE. Mitigation strategies include compositional engineering (Cs^+, Rb^+ incorporation), grain boundary passivation, and 2D capping layers (Eames et al., 2015; Khadka et al., 2021; Yuan & Huang, 2016; Zai et al., 2021). **SRH recombination** takes place at perovskite/ETL and perovskite/HTL interfaces, driven by unpassivated surface defects such as Pb^0 clusters, under-coordinated

halides, and oxygen vacancies. These defects introduce deep trap states that capture photocarriers, causing energy loss via phonon emission and reduced V_{oc}, leading to decreased V_{oc}, FF, and device efficiency. Mitigation strategies include surface passivation (organic ammonium salts, 2D capping layers), SAMs, band alignment optimization, and defect healing (Adhikari et al., 2025; P. Chen et al., 2024; Luo et al., 2020; Y. Xu et al., 2025). **Chemical corrosion and volatilization** occur at the perovskite/electrode interface and within the bulk perovskite, driven by thermal stress, moisture ingress, oxygen, and illumination. Key processes include I_2, HI, and CH_3NH_2 gas evolution; AgI and AlI_3 formation at metal contacts; δ-phase formation (δ-$FAPbI_3$, PbI_2); and Li-TFSI hygroscopicity. These phenomena cause increased R_s, irreversible performance loss, and delamination. Mitigation strategies include encapsulation with barrier layers, I_2 adsorbents (supramolecular macrocycles), dopant-free HTLs, and stable metal electrodes (Au, Cr) (Guerrero et al., 2016; W. Li et al., 2020; Paul et al., 2026; Zhou et al., 2022). **Thermomechanical modulus mismatch** affects all interfaces, particularly perovskite/ETL and perovskite/HTL junctions, driven by diurnal thermal cycling (−40°C to 85°C per ISOS protocols) and CTE mismatch ($\alpha\_perovskite \approx 3\times10^{-5}$ vs. $\alpha\_metal\_oxide \approx 0.5\times10^{-5}$ K^{-1}). This mismatch induces shear strain, mechanical delamination, micro-cracking, and catastrophic loss of electrical contact, leading to complete device failure, shunting, and irreversible performance loss. Mitigation strategies include stress-relief interlayers, compliant contact materials, optimized module architecture, and advanced encapsulation (Akylbayeva et al., 2026; Khenkin et al., 2020; Uličná et al., 2025; Wang et al., 2026). These mechanisms form an interdependent cascade where ion migration leads to field screening, charge accumulation, interfacial recombination, chemical corrosion, and mechanical failure in a feedback loop (Boyd et al., 2018; Q. Jiang et al., 2023; Ni et al., 2022; Thiesbrummel et al., 2024).

3. Nanomaterial-Based Electron Transport Layers (ETLs)

The strategic deployment of an efficient electron transport layer (ETL) is predicated not merely on structural passivity, but on fine-tuning the energy band alignment at the heterojunction to favor downhill electron extraction while providing a robust energetic barrier against minority holes. While conventional bulk metal oxides have historically driven baseline advancements, transition metal oxides engineered at the nanoscale offer a dynamic platform for manipulating electronic structures. As argued across key optoelectronic studies, the systematic alignment of frontier molecular orbitals at the perovskite/CTL interface remains the central mechanism governing efficient carrier collection and the suppression of non-radiative interface recombination channels (W.-J. Yin, Gu, & Gong, 2020; X. Yin, Guo, Xie, Que, & Kong, 2019).

The widespread replacement of TiO_2 by SnO_2 in high-efficiency n-i-p devices stems from the latter's superior band alignment and suppressed photocatalytic activity, which collectively mitigate UV-induced degradation (Q. Jiang, Zhang, & You, 2018; S. Liu et al., 2024). Yet we must ask: is this substitution a definitive solution or merely an incremental improvement? ZnO, for instance, offers comparable electron mobility to SnO_2 but suffers from chemical incompatibility with acidic perovskite precursors, leading to interfacial decomposition and rapid performance loss (S. Liu et al., 2024) . This chemical fragility, often overlooked in early reports, highlights the importance of considering not only electronic alignment but also chemical robustness when selecting ETL materials. The community has thus converged on SnO_2 as the current workhorse, though this consensus does not imply that the material is without profound limitations.

3.1 SnO_2 Quantum Dots and Nanoparticles

Colloidal SnO_2 quantum dots (QDs) and nanoparticles have largely replaced conventional TiO_2 templates in high-efficiency n-i-p architectures due to optimized band alignment and accelerated electron extraction kinetics (Q. Jiang et al., 2018; S. Liu et al., 2024). Reducing the crystalline dimensions of SnO_2 into the quantum-confined regime (2–4 nm) induces an upward shift in the conduction band minimum (CBM). First-principles density functional theory calculations confirm that low Mg doping concentrations shift the SnO_2 CBM upward to enhance the open-circuit voltage, whereas elevated dopant concentrations introduce detrimental interstitial defects (Sannino et al., 2023). This quantum-induced energetic modulation aligns the CBM of the electron transport layer with that of the metal halide perovskite, enabling efficient electron extraction with minimized thermalization and energy loss penalties (M. Kim et al., 2022).

What makes this energetic engineering particularly elegant is its intrinsic tunability: the CBM of SnO_2 QDs can be systematically adjusted through size control, enabling precise alignment with the specific perovskite composition without resorting to complex doping schemes. However, the prevailing assumption that quantum confinement alone guarantees optimal performance overlooks the critical role of surface chemistry. As we have

learned from extensive experience with semiconductor QDs, the electronic benefits of reduced dimensions are often offset by increased surface-to-volume ratios that introduce deep trap states.

Recent material strategies have focused heavily on tuning these absolute CBM and valence band maximum (VBM) positions through the incorporation of graphene quantum dots (GQDs), structural dopants, and strategic molecular interlayers (H. Li et al., 2024; Lu, Zhang, Jiang, Zhang, & Ni, 2021; Youssef et al., 2022) . The introduction of aminomethyl phosphonic acid (AMPA) as a multifunctional additive in SnO_2 ETLs has been shown to effectively passivate oxygen vacancies on the SnO_2 surface, enhance carrier mobility and crystallinity, and upward-regulate the CBM for favorable energy level alignment with the perovskite layer (Gao et al., 2025) . Incorporating GQDs or passivating chemical additives accelerates intra-layer charge transfer and substantially decreases carrier accumulation at the boundary. From an energetic perspective, the CBM of the modified SnO_2 matrix operates as a downward thermodynamic gate for electron extraction, while its exceptionally deep-lying VBM establishes an effective hole-blocking barrier, preventing parasitic minority-carrier leakage and subsequent interfacial recombination as conceptualized in Figure 2a (Q. Jiang et al., 2018; Ren et al., 2017) .

3.1.1 Surface Defects and Stability Challenges

Pristine SnO_2 QD films are intrinsically prone to surface defect densities, specifically under-coordinated tin sites and reactive surface hydroxyl groups (–OH) that operate as severe sub-gap trap states (Wang et al., 2026) . These hydroxyl species are particularly insidious: they not only trap charge carriers but also catalyze the hydrolysis of the adjacent perovskite layer, initiating a cascade of chemical degradation that undermines long-term stability. Density functional theory calculations have classified iodine interstitials (Ii) as the most easily formed harmful defects at SnO_2/perovskite interfaces, with the CBM offset measured at 0.07 eV for PbI_2/SnO_2 interfaces and 0.28 eV for MAI/SnO_2 interfaces under stress conditions (Pu, Xiao, Wang, Li, & Wang, 2022) .

Interface modification using organic additives such as polyacrylic acid (PAA) shells or PFN-Br interfacial layers mitigates these liabilities by neutralizing trap states and reducing the localized photocatalytic activity of the oxide backbone. The SnO_2/PFN-Br ETL, combined with guanidinium iodide doping, has delivered power conversion efficiencies exceeding 21% with negligible current-voltage hysteresis (Pu et al., 2022). While this hydrogen-bonding passivation effectively stiffens the Pb–I lattice and suppresses iodine vacancy formation , (Pu et al., 2022) its long-term effectiveness under simultaneous thermal and illumination stress remains questionable, as hydrogen bonds are susceptible to cleavage at elevated temperatures (>85°C). This trade-off between passivation strength and thermal stability demands urgent investigation. Furthermore, the reliance on organic interfacial layers reintroduces the very degradation pathways that all-inorganic ETLs were designed to eliminate, raising fundamental questions about the long-term viability of this approach.

3.1.2 The Scalability Bottleneck

Despite these advances, the translation of SnO_2 QD-based ETLs from lab-scale devices ($\leq$1 cm²) to large-area modules remains challenged by thickness nonuniformity and dewetting during solution processing, issues that demand further investigation into scalable deposition protocols. The very properties that make QDs attractive—their colloidal stability and size tunability—become liabilities when attempting to deposit uniform films over square-meter areas. Slot-die coating and inkjet printing have shown promise, but the relationship between processing parameters and film quality remains poorly understood for SnO_2 QD dispersions. The field must confront a sobering reality: a material that performs admirably on small-area substrates may fail catastrophically when scaled, not because of fundamental electronic limitations, but because of processing physics that are rarely considered in academic studies.

4. Nanomaterial-Based Hole Transport Layers (HTLs)

Achieving stable, long-term operational lifetimes without sacrificing high fill factors demands p-type selective matrices that provide favorable energetic cross-linking with the perovskite valence band. Nano-engineered inorganic p-type alternatives offer a path away from the degradation risks associated with conventional doped organic layers, providing robust alternatives for inverted and regular architectural configurations (Foo et al., 2022; X. Liu et al., 2026).. The rationale for inorganic HTLs is compelling: organic layers such as Spiro-OMeTAD and PTAA demand hygroscopic dopants (Li-TFSI, tBP) that actively compromise device stability, and their low glass transition temperatures make them susceptible to morphological degradation under operational heating. Yet the

substitution of organic with inorganic HTLs is not a panacea; it introduces a different set of challenges that the community is only beginning to appreciate.

4.1 Crystalline NiO_x Nanoparticles

Nickel oxide (NiO_x) nanoparticles serve as a chemically robust inorganic p-type candidate owing to their intrinsic chemical stability and compatible energy levels relative to standard perovskite thin films (Icli & Ozenbas, 2018; X. Liu et al., 2023). Experimentally, the effective Fermi level (E_F) of processed NiO_x matrices ranges between –4.7 eV and –5.5 eV, a variance dictated by local stoichiometric deviations and atmospheric exposure history (Jin et al., 2020). This electronic sensitivity to processing parameters necessitates precise synthetic control to stabilize the interfacial energy alignment, thereby minimizing device performance variability and improving reproducibility across different fabrication methodologies.

Quantitative energetic evaluations reveal that the exact position of the valence band maximum is heavily dependent on the synthetic processing and structural modification routes utilized. Ultraviolet photoelectron spectroscopy measurements have established that the work function of pristine NiO_x is approximately 4.9 eV, while modification with the self-assembled monolayer MeO-2PACz increases this to 5.5 eV, corresponding to a valence band shift from –5.3 eV to –5.7 eV (Hu et al., 2026). This deeper valence band alignment substantially reduces the energetic barrier for hole extraction. Lithium doping offers another effective strategy: the initially unfavorable VBM of NiO_x shifts upward and becomes well-aligned with narrow-bandgap perovskites, with 20 mol% Li doping identified as optimal for enhanced charge extraction (Y. J. Ahn, Park, Ji, Park, & Kim, 2025). X-ray photoelectron spectroscopy analysis has confirmed that Li doping increases the concentration of Ni^{3+} states, enhancing p-type conductivity (Yang et al., 2023)

When contrasted against the baseline VBM of traditional lead-halide perovskites—which typically registers between –5.40 eV and –5.60 eV—the deeper VBM of modified NiO_x nanoparticle matrices yields an exceptionally low energetic offset (Jin et al., 2020; X. Yin et al., 2019) . This close energetic proximity accelerates hole extraction across the interface while the high conduction band minimum of the oxide backbone effectively blocks stray electrons (Icli & Ozenbas, 2018) .

4.1.1 Processing-Dependent Performance and Surface Engineering

Despite these favorable energetics, the real-world performance of NiO_x architectures depends significantly on the precise thin-film deposition and preparation methods employed (Lee et al., 2025) . High-vacuum sputtering or non-homogenized solution routes can introduce structural traps, subsurface oxidation states, or undesirable pinholes that restrict charge transport despite high bulk conductivity. The processing-structure-property relationship in NiO_x is arguably more complex than in any other inorganic HTL, demanding a level of process control that is challenging to maintain in both academic and industrial settings.

Furthermore, an unpassivated NiO_x surface can present deep localized trap states or suboptimal Fermi level alignment that promotes non-radiative interface recombination (A. Wu, Su, Zhang, Zhang, & Chen, 2025). Pristine solution-processed NiO_x HTLs have been shown to yield relatively poor photovoltaic performance—with PCEs of approximately 17.14%—primarily due to nonradiative recombination at the NiO_x/perovskite interface and mismatched energy level alignment (H. Zhang et al., 2016). Overcoming these surface boundaries requires the introduction of organic self-assembled monolayers (SAMs) or chemical dopants, which passivate reactive nickel vacancies, align the work function, and establish a highly selective, defect-free contact zone (Cheng, Li, & Zhong, 2023; L. Zhang et al., 2025).. MeO-2PACz modification has demonstrated significant improvement, boosting PCEs to 21.61% with a V_{OC} of 1.11 V, attributed to interface defect passivation and deeper work function (T. Jiang et al., 2024) . The bandgap of NiO_x remains largely unaffected by Li doping up to 8% concentration, with a slight red-shift from 3.7 eV to 3.67 eV observed at higher doping levels (Kong, Park, & Bae, 2024) .

4.1.2 The Trade-Off Between Stability and Cost

However, the introduction of SAMs arguably shifts the locus of instability from the bulk HTL to the heterointerlayer. Although SAMs enhance initial photovoltaic parameters and early-stage operational stability, their long-term durability under prolonged thermal stress remains insufficiently characterized. Crucially, the organic moiety of SAMs reintroduces the intrinsic vulnerabilities that originally motivated the transition toward

all-inorganic HTLs—specifically, limited thermal tolerance, potential desorption pathways, and chemical reactivity at the perovskite interface. This represents a fundamental material trade-off.

4.2 The Interdependent Role of ETL and HTL

The stability gains afforded by NiO_x HTLs are not independent of the ETL choice; the coupling between ion redistribution at the HTL and recombination at the ETL creates a feedback loop where degradation at one interface accelerates failure at the other (Thiesbrummel et al., 2024). This interdependence is a critical but often overlooked aspect of device engineering. When NiO_x efficiently extracts holes, it simultaneously alters the electric field distribution within the device, which in turn affects ion migration patterns at the ETL interface. The result is a coupled system where optimization of one contact must be performed in the context of the other—a fact that complicates the interpretation of studies that examine HTL or ETL performance in isolation. The perovskite community has largely treated these layers as independent variables, yet the physics of the complete device dictates otherwise.

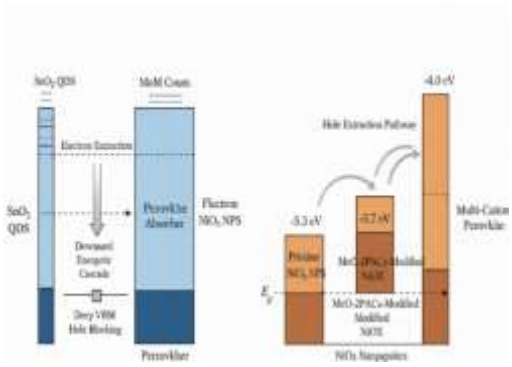

Figure 2: Schematic illustration of energy band alignment profiles at the selective contacts: (a) Quantum-confined CBM matching and hole-blocking dynamics at the modified SnO_2 QD electron-selective interface, showing the downward energetic cascade that facilitates electron extraction while the deep VBM blocks hole leakage. (b) Valence band engineering, Fermi level (E_F) position, and relative energetic extraction pathways of NiO_x NPs versus the multi-cation perovskite absorber bulk, contrasting the pristine NiO_x VBM (–5.3 eV) with the MeO-2PACz-modified NiO_x VBM (–5.7 eV).

Table 1: Functional roles and electronic configurations within the integrated band alignment schema

Material Layer	CBM (eV)	VBM (eV)	Band Gap (eV)	Work Function (eV)	Dominant Transport Function	Key References
Perovskite ($MAPbI_3$)	–3.9	–5.4	1.5	—	Photocarrier generation & ambipolar transport	Standard literature values
SnO_2 (pristine)	–4.33	—	3.6	—	Electron extraction	(Pu et al., 2022)
SnO_2 (with PFN-Br)	–3.78	—	3.6	—	Downhill electron extraction; CBM shifts to match perovskite	(Guo et al., 2020)
TiO_2	–4.2	–7.88	3.68	—	Conventional ETL baseline	Standard literature values
NiO_x (pristine)	—	–5.3	3.6–3.7	4.9	Hole extraction & electron blocking	(X. Wu et al., 2025)
NiO_x (with MeO-2PACz)	—	–5.7	~3.2	5.5	Enhanced hole extraction via SAM modification	(X. Wu et al., 2025)
NiO_x (Li-doped)	—	—	3.67–3.7	—	Improved conductivity via increased Ni^{3+} states	(Y. J. Ahn et al., 2025)
Spiro-OMeTAD (organic)	–2.2	–5.2	—	—	Conventional organic HTL baseline; limited stability	Standard literature values

5. Future Scalability, Technical Roadmap, and Concluding Perspectives

5.1 Scalable Manufacturing Protocols and Industrial Challenges

While lab-scale perovskite solar cells rely almost exclusively on spin-coating techniques to optimize small-area substrates (≤1 cm^2), the transition to commercial module manufacturing demands high-throughput, continuous roll-to-roll (R2R) operations, slot-die coating, and inkjet printing. Nano-engineered charge transport layers play an electronically active role during this deposition scaling. Solvent compatibility remains an industrial bottleneck: the chemical solvents used to process organic transport films often damage the structural integrity of the underlying perovskite layer in inverted geometries.

By contrast, inorganic nanomaterial suspensions—such as stabilized aqueous or alcoholic dispersions of SnO_2 and NiO_x nanoparticles provide a chemically benign processing window. However, large-area slot-die coating of colloidal metal oxides introduces rheological challenges, including nanoparticle agglomeration and meniscus instability, which manifest as pinholes and spatial thickness variations across the module sub-cells. This morphological nonuniformity directly induces current crowding and localized shunting, compromising the fill factor (FF) of full-sized solar modules.

5.2 Artificial Intelligence and Machine Learning Screening

Accelerating the optimization of resilient heterointerfaces requires a shift away from trial-and-error experimentation toward Machine Learning (ML)-assisted computational screening. High-throughput density functional theory (DFT) datasets can be integrated with neural network models to predict the energetic band shifting, mechanical shear modulus, and chemical binding energies of multi-component interlayers before experimental formulation (Kouroudis et al., 2024). .

ML algorithms can systematically evaluate millions of organic self-assembled monolayer (SAM) configurations on crystalline NiO_x surfaces, targeting structures that maximize the valence band alignment while establishing a hydrophobic chemical shield against ambient moisture ingress. This computational approach shortens the material discovery pipeline, directly pinpointing candidate interlayers that exhibit low defect formation energies and superior thermodynamic stability under operational conditions (Kouroudis et al., 2024).

5.3 Standardized Multi-Stress Testing Protocols (ISOS Framework)

The historical reliance on simple room-temperature shelf-life testing is fundamentally inadequate for predicting a device's decade-scale commercial lifespan. To ensure reliable cross-laboratory validation, emerging research must adhere strictly to the International Summit on Perovskite Solar Cell Stability (ISOS) protocols (Khenkin et al., 2020). Nano-engineered CTLs must be systematically evaluated under combined thermal, radiative, and electrical stressors.

Specifically, the ISOS-L-2 (continuous illumination at elevated temperatures) and ISOS-T-2 (thermal cycling from −40°C to 85°C) protocols are critical for exposing the latent vulnerabilities discussed herein, such as field-driven ion migration across grain boundaries and thermomechanical shear fatigue at the metal-oxide interface (Akylbayeva et al., 2026; Khenkin et al., 2020). Evaluating devices under isolated single-stress parameters masks the destructive feedback loops that dominate real-world operations.

Table 2: Scalability Roadmap for Nanomaterial-Based Transport Layers

Stage	Key Activities	Milestones	Key Challenges	References
Phase I (1–3 years)	Standardize ISOS protocols; develop ML databases; validate scalable deposition; identify green solvents	Consensus on minimum stability reporting; preliminary ML models for SAM screening	Data scarcity for ML; solvent compatibility with QDs; uniformity on 100 cm^2 areas	(Khenkin et al., 2020; Kouroudis et al., 2024; Lee et al., 2025)
Phase II (3–5 years)	ML-guided synthesis; hermetic ALD encapsulation; module efficiency demonstration	≥25% efficient modules (>100 cm^2); T80 >10,000 h (ISOS-L-3)	ALD throughput/cost; reproducibility of ML predictions; interfacial stability with encapsulation	(Paul et al., 2026; Uličná et al., 2025)

Phase III (5–10 years)	Green solvent processing; stress-relief architectures; self-healing interfaces	T80 >25,000 h (outdoor); 100% green solvent processing; full LCA	Self-healing material design; long-term outdoor validation; manufacturing scale-up	(Akylbayeva et al., 2026; Wang et al., 2026)

6. Conclusion and Societal Impact

This critical review has systematically evaluated the multi-dimensional stabilization roles played by nano-engineered interfaces and charge transport layers in perovskite photovoltaics. We have demonstrated that the operational longevity of these devices is governed by a complex, interdependent degradation cascade encompassing field-driven halide migration, non-radiative Shockley-Read-Hall recombination, chemical corrosion, and thermomechanical shear stress. Transitioning to quantum-confined metal oxides, such as size-tuned SnO_2 quantum dots and structurally passivated NiO_x nanoparticles, provides an effective mechanism for tuning absolute band edges, optimizing charge extraction kinetics, and establishing chemical barriers against degradation byproducts.

From a broader developmental perspective, resolving the efficiency-stability trade-off at these buried heterojunctions is essential for transitioning perovskite photovoltaics from lab-scale curiosities into a commercially viable clean energy technology. Facilitating the deployment of low-cost, high-efficiency, and structurally durable solar modules directly supports global sustainability objectives by accelerating the decarbonization of industrial power grids, reducing reliance on fossil fuels, and providing decentralized clean electricity to remote communities. Future research trajectories must unify machine-learning-assisted interface discovery, strict adherence to multi-stress ISOS protocols, and the development of eco-friendly, scalable roll-to-roll manufacturing methods to bridge the gap between academic innovation and commercial reality.

References

[1] Adhikari, R. D., Patel, M. J., Baishya, H., Yadav, D., Kalita, M., Alam, M., & Iyer, P. K. (2025). Decoding recombination dynamics in perovskite solar cells: an in-depth critical review. Chemical Society Reviews, 54(8), 3962-4034.

[2] Ahn, N., & Choi, M. (2024). Towards long-term stable perovskite solar cells: degradation mechanisms and stabilization techniques. Advanced science, 11(4), 2306110.

[3] Ahn, Y. J., Park, I. J., Ji, S. G., Park, M.-A., & Kim, J. Y. (2025). Tailoring NiOx hole transport layers by Li doping for narrow-bandgap perovskite solar cells. Journal of Alloys and Compounds, 183838.

[4] Akylbayeva, A., Nussupov, Y., Omarova, Z., Korshikov, Y., Aldiyarov, A., & Yerezhep, D. (2026). Stability and Degradation of Perovskite Solar Cells in Space Environments: Mechanisms and Protocols. International Journal of Molecular Sciences, 27(8), 3459.

[5] Berhe, T. A., Su, W.-N., Chen, C.-H., Pan, C.-J., Cheng, J.-H., Chen, H.-M., . . . Hwang, B.-J. (2016). Organometal halide perovskite solar cells: degradation and stability. Energy & Environmental Science, 9(2), 323-356.

[6] Boyd, C. C., Cheacharoen, R., Leijtens, T., & McGehee, M. D. (2018). Understanding degradation mechanisms and improving stability of perovskite photovoltaics. Chemical Reviews, 119(5), 3418-3451.

[7] Chen, J., Wang, X., Wang, T., Li, J., Chia, H. Y., Liang, H., . . . Guo, R. (2025). Determining the bonding–degradation trade-off at heterointerfaces for increased efficiency and stability of perovskite solar cells. Nature energy, 10(2), 181-190.

[8] Chen, P., Zheng, Q., Jin, Z., Wang, Y., Wang, S., Sun, W., . . . Wu, J. (2024). Buried Interface Engineering-Assisted Defects Control and Crystallization Manipulation Enables Stable Perovskite Solar Cells with Efficiency Exceeding 25%. Advanced Functional Materials, 34(49), 2409497.

[9] Cheng, H., Li, Y., & Zhong, Y. (2023). Towards cost-efficient and stable perovskite solar cells and modules: utilization of self-assembled monolayers. Materials Chemistry Frontiers, 7(18), 3958-3985.

[10] Dai, Z., & Padture, N. P. (2023). Challenges and opportunities for the mechanical reliability of metal halide perovskites and photovoltaics. Nature energy, 8(12), 1319-1327.

[11] Eames, C., Frost, J. M., Barnes, P. R., O'regan, B. C., Walsh, A., & Islam, M. S. (2015). Ionic transport in hybrid lead iodide perovskite solar cells. Nature communications, 6(1), 7497.

[12] Elnaggar, M., Boldyreva, A. G., Elshobaki, M., Tsarev, S. A., Fedotov, Y. S., Yamilova, O. R., . . . Troshin, P. A. (2020). Decoupling Contributions of Charge-Transport Interlayers to Light-Induced Degradation of p-i-n Perovskite Solar Cells. Solar RRL, 4(9), 2000191.

[13] Foo, S., Thambidurai, M., Senthil Kumar, P., Yuvakkumar, R., Huang, Y., & Dang, C. (2022). Recent review on electron transport layers in perovskite solar cells. International journal of energy research, 46(15), 21441-21451.

[14] Gao, Y., Gong, W., Zhang, Z., Guo, J., Ma, J., Li, X., . . . Wu, M. (2025). Aminomethyl phosphonic acid as highly effective multifunctional additive for modification of electron transport layer and perovskite in photovoltaic solar cells. Angewandte Chemie, 137(23), e202424479.

[15] Gong, J., Cui, Y., Li, F., & Liu, M. (2023). Progress in surface modification of SnO2 electron transport layers for stable perovskite solar cells. Small Science, 3(6), 2200108.

[16] Guerrero, A., You, J., Aranda, C., Kang, Y. S., Garcia-Belmonte, G., Zhou, H., . . . Yang, Y. (2016). Interfacial degradation of planar lead halide perovskite solar cells. ACS nano, 10(1), 218-224.

[17] Guo, Y., Lei, H., Wang, C., Ma, J., Chen, C., Zheng, X., . . . Tan, Z. (2020). Reconfiguration of Interfacial and Bulk Energy Band Structure for High-Performance Organic and Thermal–Stability Enhanced Perovskite Solar Cells. Solar RRL, 4(4), 1900482.

[18] Hermes, I. M., Hou, Y., Bergmann, V. W., Brabec, C. J., & Weber, S. A. (2018). The interplay of contact layers: How the electron transport layer influences interfacial recombination and hole extraction in perovskite solar cells. The journal of physical chemistry letters, 9(21), 6249-6256.

[19] Hu, Q., He, Z., Wang, G., Pu, Y., Yang, Q., Zuo, Y., . . . Wang, J. (2026). Intermolecular Coupling Reinforces Self-Assembled Hole-Transport Layers Stability and Performance in NiOx-Based Inverted Perovskite Solar Cells. Advanced Functional Materials, e26993.

[20] Icli, K. C., & Ozenbas, M. (2018). Fully metal oxide charge selective layers for nip perovskite solar cells employing nickel oxide nanoparticles. Electrochimica Acta, 263, 338-345.

[21] Jiang, Q., Tirawat, R., Kerner, R. A., Gaulding, E. A., Xian, Y., Wang, X., . . . Zhu, K. (2023). Towards linking lab and field lifetimes of perovskite solar cells. Nature, 623(7986), 313-318.

[22] Jiang, Q., Zhang, X., & You, J. (2018). SnO2: a wonderful electron transport layer for perovskite solar cells. Small, 14(31), 1801154.

[23] Jiang, T., Yang, Y., Hao, X., Fan, J., Wu, L., Wang, W., . . . Zhang, J. (2024). Self-assembled monolayer hole transport layers for high-performance and stable inverted perovskite solar cells. Energy & Fuels, 38(21), 21371-21381.

[24] Jin, Z., Guo, Y., Yuan, S., Zhao, J.-S., Liang, X.-M., Qin, Y., . . . Ai, X.-C. (2020). Modification of NiO x hole transport layer for acceleration of charge extraction in inverted perovskite solar cells. RSC advances, 10(21), 12289-12296.

[25] Khadka, D. B., Shirai, Y., Yanagida, M., & Miyano, K. (2021). Insights into accelerated degradation of perovskite solar cells under continuous illumination driven by thermal stress and interfacial junction. ACS Applied Energy Materials, 4(10), 11121-11132.

[26] Khenkin, M. V., Katz, E. A., Abate, A., Bardizza, G., Berry, J. J., Brabec, C., . . . Di Carlo, A. (2020). Consensus statement for stability assessment and reporting for perovskite photovoltaics based on ISOS procedures. Nature energy, 5(1), 35-49.

[27] Kim, K. W., Seo, Y.-H., Ann, M. H., Lee, W., Nam, J., Chung, J., . . . Kim, T.-S. (2024). Overcoming stability limitations of efficient, flexible perovskite solar modules. Joule, 8(5), 1380-1393.

[28] Kim, M., Jeong, J., Lu, H., Lee, T. K., Eickemeyer, F. T., Liu, Y., . . . Kim, H.-B. (2022). Conformal quantum dot–SnO2 layers as electron transporters for efficient perovskite solar cells. Science, 375(6578), 302-306.

[29] Kong, M.-S., Park, M.-S., & Bae, S.-Y. (2024). Post-growth annealing effect of Li-doped NiO thin films grown by mist chemical vapor deposition. Materials Science and Engineering: B, 310, 117736.

[30] Kouroudis, I., Tanko, K. T., Karimipour, M., Ali, A. B., Kumar, D. K., Sudhakar, V., . . . Gagliardi, A. (2024). Artificial intelligence-based, wavelet-aided prediction of long-term outdoor performance of perovskite solar cells. ACS energy letters, 9(4), 1581-1586.

[31] Kung, P. K., Li, M. H., Lin, P. Y., Chiang, Y. H., Chan, C. R., Guo, T. F., & Chen, P. (2018). A review of inorganic hole transport materials for perovskite solar cells. Advanced Materials Interfaces, 5(22), 1800882.

[32] Lee, H., Jung, H. R., Pak, S., Kwon, N., Kim, S. H., Na, J., . . . Jeong, J.-h. (2025). Unveiling NiO x/Perovskite Interfaces: Charge Transport and Device Performance in Perovskite Solar Cells. ACS Applied Materials & Interfaces, 17(37), 52263-52275.

[33] Li, H., Xu, J., Han, J., Lan, Q., Wu, Z., Xie, M., . . . Wang, J. (2024). Ammonium iodide-incorporated SnO2 obtains perovskite solar cells with over 24% efficiency. Applied Physics Letters, 124(12).

[34] Li, W., Lai, X., Meng, F., Li, G., Wang, K., Kyaw, A. K. K., & Sun, X. W. (2020). Efficient defect-passivation and charge-transfer with interfacial organophosphorus ligand modification for enhanced performance of perovskite solar cells. Solar energy materials and solar cells, 211, 110527.

[35] Liu, N., Zhang, L., Liang, Y., Xue, B., & Wang, D. (2023). Effects of carrier transport layers on performance degradation in perovskite solar cells under proton irradiation. ACS Applied Energy Materials, 6(12), 6673-6680.

[36] Liu, S., Luan, F., Wu, Z., Shou, C., Xie, H., & Yang, S. (2024). In-situ Growth of Conformal SnO 2 Layers for Efficient Perovskite Solar Cells. Journal of Inorganic Materials, 39(12), 1397-1403.

[37] Liu, X., Gong, J., Xue, B., Bu, T., Cheng, Y. B., & Huang, F. (2026). Inorganic Charge Transport Layers for High-Performance p-i-n Perovskite Solar Cells. ChemSusChem, 19(1), e202501739.

[38] Liu, X., Liu, Y., Lang, R., Liu, Y., Lei, W., Cong, R., . . . Wang, X. (2023). Optimizing the Performance of Sputtered-NiOx-Based Perovskite Solar Cells via Regulating the PbI2 Concentration. Energy Technology, 11(9), 2300355.

[39] Lu, C., Zhang, W., Jiang, Z., Zhang, Y., & Ni, C. (2021). Graphene quantum dots doping SnO2 for improving carrier transport of perovskite solar cells. Ceramics International, 47(21), 29712-29721.

[40] Luo, D., Su, R., Zhang, W., Gong, Q., & Zhu, R. (2020). Minimizing non-radiative recombination losses in perovskite solar cells. Nature Reviews Materials, 5(1), 44-60.

[41] Nazir, G., Lee, S. Y., Lee, J. H., Rehman, A., Lee, J. K., Seok, S. I., & Park, S. J. (2022). Stabilization of perovskite solar cells: recent developments and future perspectives. Advanced Materials, 34(50), 2204380.

[42] Ni, Z., Jiao, H., Fei, C., Gu, H., Xu, S., Yu, Z., . . . Liu, Y. (2022). Evolution of defects during the degradation of metal halide perovskite solar cells under reverse bias and illumination. Nature energy, 7(1), 65-73.

[43] Paul, G., Schall, J. W., Guthrey, H. L., Migliozzi, M., Tirawat, R., Roberts, D. M., . . . Palmstrom, A. F. (2026). Multiscale Characterization of Electrode-Induced Degradation in Perovskite Solar Cells. ACS Applied Energy Materials, 9(5), 2503-2512.

[44] Pu, W., Xiao, W., Wang, J., Li, X.-W., & Wang, L. (2022). Stress and defect effects on electron transport properties at SnO2/Perovskite interfaces: A first-principles insight. ACS omega, 7(18), 16187-16196.

[45] Qin, J., Che, Z., Kang, Y., Liu, C., Wu, D., Yang, H., . . . Zhan, Y. (2024). Towards operation-stabilizing perovskite solar cells: fundamental materials, device designs, and commercial applications. InfoMat, 6(4), e12522.

[46] Ren, X., Yang, D., Yang, Z., Feng, J., Zhu, X., Niu, J., . . . Liu, S. F. (2017). Solution-processed Nb: SnO2 electron transport layer for efficient planar perovskite solar cells. ACS Applied Materials & Interfaces, 9(3), 2421-2429.

[47] Sannino, G. V., Pecoraro, A., Maddalena, P., Bruno, A., Veneri, P. D., Pavone, M., & Muñoz-García, A. B. (2023). The role of Mg dopant concentration in tuning the performance of the SnO 2 electron transport layer in perovskite solar cells. Sustainable Energy & Fuels, 7(19), 4855-4863.

[48] Shen, Y., Li, C., Liu, C., Reitz, S. A., Chen, B., & Sargent, E. H. (2024). The impact of interface and heterostructure on the stability of perovskite-based solar cells. Applied Physics Reviews, 11(4).

[49] Shi, Y., Hu, W., Yue, Q., Lin, Z., Zhang, B., Jiang, S., . . . Han, H. (2026). Practical Interfaces for High-Performance Perovskite Solar Cells. Solar RRL, 10(1), e202500925.

[50] Thiesbrummel, J., Shah, S., Gutierrez-Partida, E., Zu, F., Peña-Camargo, F., Zeiske, S., . . . Brinkmann, K. O. (2024). Ion-induced field screening as a dominant factor in perovskite solar cell operational stability. Nature energy, 9(6), 664-676.

[51] Tirawat, R., Louks, A. E., Yang, M., Habisreutinger, S. N., van de Lagemaat, J., Uličná, S., . . . Palmstrom, A. F. (2024). Measuring metal halide perovskite single cell degradation consistent with module-based conditions. Sustainable Energy & Fuels, 8(3), 546-553.

[52] Ulicna, S., Schall, J. W., Hayden, S. C., Irvin, N. P., Silverman, T. J., Fei, C., . . . Parker, J. (2025). Field-Relevant Degradation Mechanisms in Metal Halide Perovskite Modules. Advanced Energy Materials, 15(23).

[53] Uličná, S., Schall, J. W., Hayden, S. C., Irvin, N. P., Silverman, T. J., Fei, C., . . . Parker, J. (2025). Field-Relevant Degradation Mechanisms in Metal Halide Perovskite Modules. Advanced Energy Materials, 15(23), 2404518.

[54] Wang, H., Liu, C., Xu, R., Zhang, Y., De Wolf, S., & Wang, K. (2026). Upper Interface Engineering Between Perovskite and Electron Transport Layer Toward Efficient and Stable Inverted Perovskite Solar Cells. Advanced Materials, 38(5), e13633.

[55] Wei, J., Wang, Q., Huo, J., Gao, F., Gan, Z., Zhao, Q., & Li, H. (2021). Mechanisms and suppression of photoinduced degradation in perovskite solar cells. Advanced Energy Materials, 11(3), 2002326.

[56] Wu, X., Yang, H., Yue, Z., Wang, Y., Liu, M., Zeng, J., . . . Ding, L. (2025). Hydroxyl-driven homogeneous and robust SAM anchoring on NiOx for high-performance inverted perovskite solar cells. Chemical Engineering Journal, 166008.

[57] Wu, Y., Li, W., Li, S., Niu, Y. F., Wang, C., Yang, H. B., . . . Shi, X. (2026). Supramolecular Macrocyclic Iodine Adsorbents Enable Photothermally Stable Perovskite Solar Cells. Advanced science, 13(4), e16964.

[58] Xu, Y., Yu, J., Liu, S., Tang, F., Ma, N., Zhang, K., & Huang, F. (2025). Surface potential homogenization improves perovskite solar cell performance. Advanced Energy Materials, 15(12), 2404755.

[59] Xu, Z., Kerner, R. A., Kronik, L., & Rand, B. P. (2024). Beyond ion migration in metal halide perovskites: toward a broader photoelectrochemistry perspective. ACS energy letters, 9(9), 4645-4654.

[60] Yang, M., Zhu, X., Mo, K., Li, S., Cheng, S., Liu, Y., . . . Wang, Z. (2023). Tuning surface oxidation states of nickel oxide for efficient inverted perovskite solar cells. ACS Applied Energy Materials, 6(3), 1332-1339.

[61] Yin, W.-J., Gu, H.-J., & Gong, X.-G. (2020). Computational Modeling and the Design of Perovskite Solar Cells Handbook of Materials Modeling: Applications: Current and Emerging Materials (pp. 2849-2864): Springer.

[62] Yin, X., Guo, Y., Xie, H., Que, W., & Kong, L. B. (2019). Nickel oxide as efficient hole transport materials for perovskite solar cells. Solar RRL, 3(5), 1900001.

[63] You, J., Meng, L., Song, T.-B., Guo, T.-F., Yang, Y., Chang, W.-H., . . . Chen, Q. (2016). Improved air stability of perovskite solar cells via solution-processed metal oxide transport layers. Nature nanotechnology, 11(1), 75-81.

[64] Youssef, R. M., Salem, A., Shawky, A., Ebrahim, S., Soliman, M., Abdel-Mottaleb, M. S., & El-Sheikh, S. M. (2022). Solution-processed quantum dot SnO2 as an interfacial electron transporter for stable fully-air-fabricated metal-free perovskite solar cells. Journal of Materiomics, 8(6), 1172-1183.

[65] Yuan, Y., & Huang, J. (2016). Ion migration in organometal trihalide perovskite and its impact on photovoltaic efficiency and stability. Accounts of chemical research, 49(2), 286-293.

[66] Zai, H., Ma, Y., Chen, Q., & Zhou, H. (2021). Ion migration in halide perovskite solar cells: Mechanism, characterization, impact and suppression. Journal of Energy Chemistry, 63, 528-549.

[67] Zang, L., Zhao, C., Hu, X., Tao, J., Chen, S., & Chu, J. (2024). Emerging trends in electron transport layer development for stable and efficient perovskite solar cells. Small, 20(26), 2400807.

[68] Zhang, H., Cheng, J., Lin, F., He, H., Mao, J., Wong, K. S., . . . Choy, W. C. (2016). Pinhole-free and surface-nanostructured NiO x film by room-temperature solution process for high-performance flexible perovskite solar cells with good stability and reproducibility. ACS nano, 10(1), 1503-1511.

[69] Zhang, L., Wang, C., Wei, Y., Chen, J., Xin, H., Zhang, H., . . . Wu, X. (2025). Electronic Effect of Self-Assembled Molecules on Buried Interface Recombination in nip Perovskite Solar Cells. ACS Applied Materials & Interfaces, 17(28), 41342-41349.

[70] Zhao, X., Liu, T., Burlingame, Q. C., Liu, T., Holley III, R., Cheng, G., . . . Loo, Y.-L. (2022). Accelerated aging of all-inorganic, interface-stabilized perovskite solar cells. Science, 377(6603), 307-310.

[71] Zhou, Q., Duan, J., Duan, Y., & Tang, Q. (2022). Review on engineering two-dimensional nanomaterials for promoting efficiency and stability of perovskite solar cells. Journal of Energy Chemistry, 68, 154-175.